Journal of
Applied Sciences

Virtual Study of Natural Convection Heat Transfer in an Inclined Square Cavity

C.S. Nor Azwadi, M.Y. Mohd Fairus and S. Syahrullail
Faculty of Mechanical Engineering, Universiti Teknologi Malaysia, 81310 UTM, Skudai, Johor, Malaysia

Abstract: This study presented numerical prediction of natural convection heat transfer inside an inclined square cavity with perfectly conducting boundary conditions for the top and bottom walls. The modified Navier Stokes equations were solved using finite difference approach with uniform mesh resolution. The inclination angels were varied from 0° to 90° with 20° intervals. The results were presented in terms of streamlines and isotherms plots. The detailed heat transfer mechanism based on the average Nusselt number and inclination angles are presented. The effects of the boundary conditions on the sidewalls on the flow behavior are also demonstrated numerically.

Key words: Natural convection, heat transfer, inclination angle, finite difference, nusselt number

INTRODUCTION

The natural convection heat transfer inside a cavity has attracted many early studies (Lee and Hellman, 1969; Clifton and Chapman, 1969; Hassan and Mohamed, 1970; Rasoul and Prinos, 1997) with the main concern to understand the heat transfer mechanism and fluid flow characteristic around the surface (Qi, 2008). Currently, the natural convection plays important roles in many science and engineering applications such as casting solidification process, cooling of electrical components, solar collecting and heating-ventilating process. The fact that the velocity and the temperature equations are solved simultaneously makes the study of natural convection quite complex (Das and Reddy, 2006; Azwadi and Tanahashi, 2007). Among the studies on natural convection phenomenon inside an enclosed cavity that are thoroughly reviewed by Ostrach (1988) many are applying adiabatic boundary conditions for top and bottom walls but very few are having perfectly conducting walls despite its importance in real engineering application (Oosthuizen and Naylor, 1998; Bubvonich *et al.*, 2002). The importance of the wall boundary condition is affirmed by the study by Kim and Viskanta (1984), who claimed that besides the flow characteristic, the thermal and the geometrical characteristic of the walls are also affecting the Nusselt number (Kim and Viskanta, 1984; Ha *et al.*, 2002). To the best of researchers knowledge, only Yucel and Ozdem (2003) conducted investigations with perfectly conducting sidewalls and a variation of the mean Nusselt number with the Rayleigh number.

There are many types of geometrical configurations have being applied to better understand the phenomenon of natural convection in a cavity. Among those that have been demonstrated are the central conducting block (Azwadi and Tanahashi, 2008; Sun and Amery, 1997; Ha and Jung, 2000), the partial dividers (Yucel and Ozdem, 2003; Ha and Jung, 2000) and the different positions of the differentially heated walls (Kim and Viskanta, 1984). The effect of inclined cavity on the heat transfer characteristic has been investigated by Das and Reddy (2006), who figured out that for an air in an enclosed system, the Rayleigh number above 10^3 will display a distinctive change in the convection heat transfer rate as the inclination angle increased. In the present simulation, we extend the value of Rayleigh number up to 10^5 and investigate the effect on the convection as the inclination angle varied. Since, the inclined cavity study by Das and Reddy (2006) is done along with a central conducting block and adiabatic sidewalls, the present study is differentiated in terms of the absence of the heat source inside the cavity and the perfectly conducting side walls.

There are plenty of early studies on the effect of inclination angle on the natural convection heat transfer in an enclosed cavity. The earliest result reported the stability analysis of the flow by Hart (1971). An experiment by Hiroyuki *et al.* (1974) to estimate the flow characteristic, Nusselt number and critical Rayleigh number revealed that the Rayleigh number at 10^4 gives the minimum and the maximum heat transfer rate as the angle increases. Besides that, Kuyper *et al.* (1993) claimed that the heat flux is strongly dependent on the Rayleigh number and inclination angle through the experiment which is done in the range of 10^4 to 10^6 Rayleigh number.

Corresponding Author: C.S. Nor Azwadi, Faculty of Mechanical Engineering, University Teknologi Malaysia,
81310 UTM, Skudai, Johor, Malaysia

In the present study, we predicted a natural convection heat transfer phenomenon in an enclosed inclined cavity by solving the modified Navier-Stokes equations and discretised using the finite difference approach. The aspect ratio was fixed to unity as we varied the inclination angle of the cavity. The sidewalls were maintained at different hot temperature and cold temperature while the top and bottom walls were set at perfectly conducting boundary condition. As far as the flow, we assumed a two dimensional, steady and laminar flow across the calculation domain. The objective of the present numerical study was to investigate the effect of inclination angle on the natural heat convection inside a perfectly conducting top and bottom walls cavity.

PROBLEM PHYSICS AND BOUNDARY CONDITIONS

In the present numerical study, the simulation was done at five different angels between 20° to 90°. As far as the fluid characteristic, the Prandlt number of 0.71 was used to represent circulation of air in the system. Furthermore, the Boussinesq approximation was included in the buoyancy force term so that all densities are assumed constant in the body force term except the one in the gravity term which changes with temperature. So, the body force term in x and y direction become:

$$G_x = \beta g_0 (T - T_m)_i$$
$$G_y = \beta g_0 (T - T_m)_j \qquad (1)$$

The dimensionless numbers used in the fluid flow calculation are the Prandtl and Rayleigh numbers defined as follow:

$$Pr = \frac{\upsilon}{\chi} \qquad (2)$$

$$Ra = \frac{\rho \beta (T_H - T_C) L^3}{\upsilon \chi} \qquad (3)$$

The geometry being solved in this study is shown in Fig. 1. The length of each side of the cavity is L and the hot wall is inclined with an angle of φ with the horizontal axis. The wall opposite to the hot wall is maintained at cold temperature while the other two walls (bottom and top walls) are set at perfectly conducting boundary condition defined as followed:

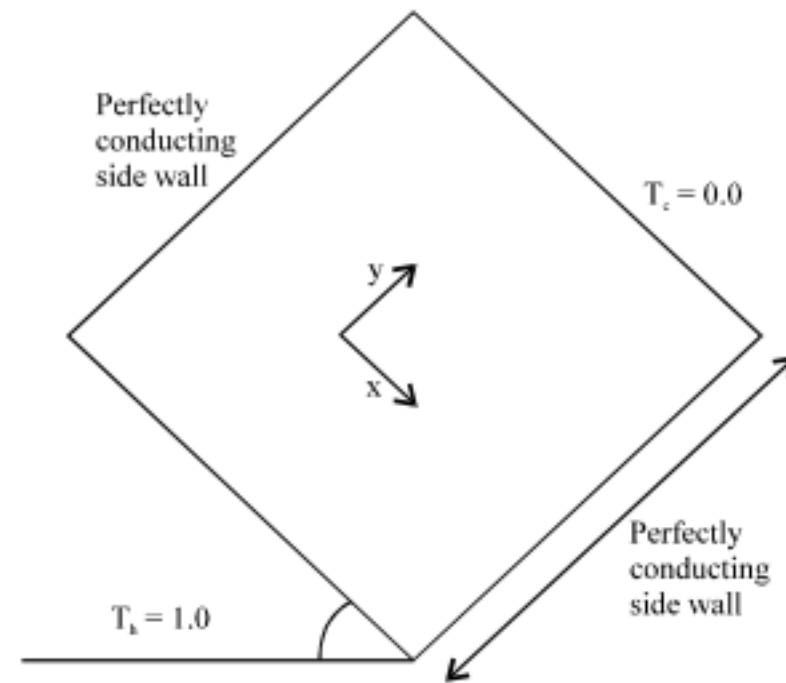$$T = T_h - \left(\frac{x}{L}\right)(T_h - T_c) \qquad (4)$$

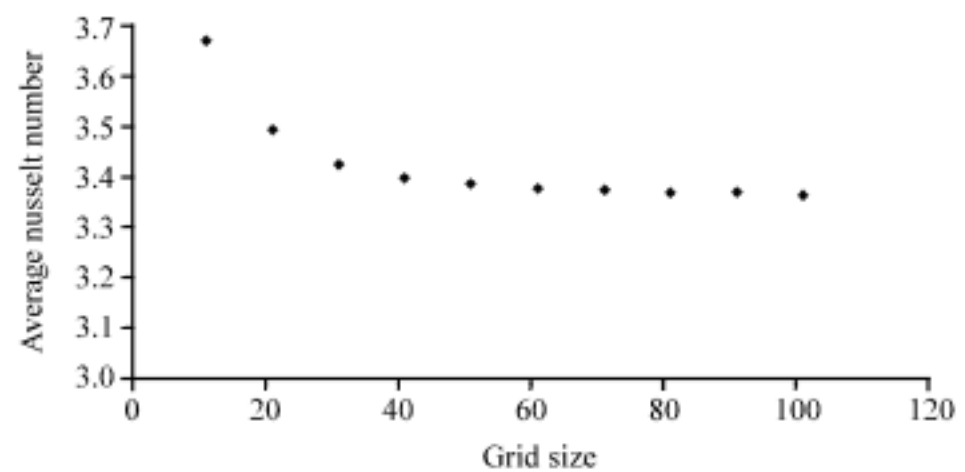Fig. 1: Geometry of the case study

Fig. 2: Grid dependence test

For verifying the grid independence of the predicted results, a grid resolution study has been carried out and shown in Fig. 2, at an inclination angle of 90° and Rayleigh number of 10^5. The differences were found to be minor, for grid refinement from 81×81 to 101×101. Hence in the present simulation, a 101×101 grid has been used for all the cases studied.

NUMERICAL MODEL

In this study, the incompressible, laminar and two-dimensional Navier Stokes equations along with the continuity and energy equations are solved in terms of stream function and vorticity. Then, the finite difference approach will be applied to discretize the equations. The governing equations used in the present study are as followed:

$$\frac{\partial u}{\partial x} + \frac{\partial v}{\partial y} = 0 \qquad (5)$$

$$u \frac{\partial u}{\partial x} + v \frac{\partial u}{\partial y} = -\frac{1}{\rho} \frac{\partial P}{\partial x} + \upsilon \left(\frac{\partial^2 u}{\partial x^2} + \frac{\partial^2 u}{\partial y^2}\right) + \beta g \cos \phi (T - T_l) \qquad (6)$$

$$u\frac{\partial v}{\partial x}+v\frac{\partial v}{\partial y}=-\frac{1}{\rho}\frac{\partial P}{\partial y}+\upsilon\left(\frac{\partial^2 v}{\partial x^2}+\frac{\partial^2 v}{\partial y^2}\right)+\beta g\sin\phi(T-T_1) \quad (7)$$

$$u\frac{\partial T}{\partial x}+v\frac{\partial T}{\partial y}=\left(\frac{k}{\rho C_p}\right)\left(\frac{\partial^2 T}{\partial x^2}+\frac{\partial^2 T}{\partial y^2}\right) \quad (8)$$

Next, the pressure terms are removed by taking the y-derivative of Eq 6 and subtracting from the x-derivative of Eq. 7. The resulting equation is:

$$u\left(\frac{\partial^2 v}{\partial x^2}-\frac{\partial^2 u}{\partial x\partial y}\right)+v\left(\frac{\partial^2 v}{\partial x\partial y}-\frac{\partial^2 u}{\partial y^2}\right)+\frac{\partial v}{\partial x}\left(\frac{\partial u}{\partial x}+\frac{\partial v}{\partial y}\right)-\frac{\partial u}{\partial y}\left(\frac{\partial u}{\partial x}+\frac{\partial v}{\partial y}\right)= $$
$$\upsilon\left[\left(\frac{\partial^3 v}{\partial x^3}-\frac{\partial^3 u}{\partial x^2\partial y}\right)+\left(\frac{\partial^3 v}{\partial y^2\partial x}-\frac{\partial^3 u}{\partial y^3}\right)\right]-\beta g\left(\frac{\partial T}{\partial y}\cos\phi-\frac{\partial T}{\partial x}\sin\phi\right) \quad (9)$$

The vorticity and stream function equation

$$\omega=\left(\frac{\partial v}{\partial x}-\frac{\partial u}{\partial y}\right) \quad (10)$$

$$u=\frac{\partial\psi}{\partial y}, v=-\frac{\partial\psi}{\partial x} \quad (11)$$

is then be applied in Eq. 9 to rewrite the equation in term of vorticity, ω

$$u=\frac{\partial\omega}{\partial x}+\frac{\partial\omega}{\partial y}=\upsilon\left(\frac{\partial^2\omega}{\partial x^2}+\frac{\partial^2\omega}{\partial y^2}\right)+\beta g\left[\frac{\partial T}{\partial x}\sin\phi-\frac{\partial T}{\partial y}\cos\phi\right] \quad (12)$$

and plugging in the stream function, ψ, Eq. 12 becomes:

$$\frac{\partial\psi}{\partial y}\frac{\partial\omega}{\partial x}-\frac{\partial\psi}{\partial x}\frac{\partial\omega}{\partial y}=\upsilon\left(\frac{\partial^2\omega}{\partial x^2}+\frac{\partial^2\omega}{\partial y^2}\right)+\beta g\left[\frac{\partial T}{\partial x}\sin\phi-\frac{\partial T}{\partial y}\cos\phi\right] \quad (13)$$

In term of the stream function, Eq. 8 and 10 can be defined as:

$$-\omega=\left(\frac{\partial^2\psi}{\partial x^2}+\frac{\partial^2\psi}{\partial y^2}\right) \quad (14)$$

$$\frac{\partial\psi}{\partial y}\frac{\partial T}{\partial x}+\frac{\partial\psi}{\partial x}\frac{\partial T}{\partial y}=\left(\frac{k}{\rho C_p}\right)\left(\frac{\partial^2 T}{\partial x^2}+\frac{\partial^2 T}{\partial y^2}\right) \quad (15)$$

Before the discretization process, we introduce the following dimensionless variables:

$$\Psi=\frac{\psi Pr}{\upsilon}, \Omega=\frac{\omega L^2 Pr}{\upsilon}, X=\frac{x}{L}, Y=\frac{y}{L}, \theta=\frac{T-T_c}{T_h-T_c} \quad (16)$$

In term of these dimensionless variables, Eq. 13-15 become:

$$\frac{\partial^2\Omega}{\partial X^2}+\frac{\partial^2\Omega}{\partial Y^2}=\frac{1}{Pr}\left(\frac{\partial\Psi}{\partial Y}\frac{\partial\Omega}{\partial X}-\frac{\partial\Psi}{\partial X}\frac{\partial\Omega}{\partial Y}\right)-Ra\left[\frac{\partial\theta}{\partial X}\sin\phi-\frac{\partial\theta}{\partial Y}\cos\phi\right] \quad (17)$$

$$-\Omega=\left(\frac{\partial^2\Psi}{\partial X^2}+\frac{\partial^2\Psi}{\partial Y^2}\right) \quad (18)$$

$$\frac{\partial\Psi}{\partial Y}\frac{\partial\theta}{\partial X}+\frac{\partial\Psi}{\partial X}\frac{\partial\theta}{\partial Y}=\left(\frac{\partial^2\theta}{\partial X^2}+\frac{\partial^2\theta}{\partial Y^2}\right) \quad (19)$$

Finally, the second order finite difference is applied to Eq. 17-19 and the solutions are obtained in term of stream function and temperature. At the end of the computations, the average Nusselt number is also calculated along the hot and cold walls.

RESULTS AND DISCUSSION

We have set up the physical problem and the calculation domain. We then derived the mathematical model to solve the natural convection problem before proceeding with the discretization process using the finite difference scheme. Here, the predicted numerical results will be discussed in terms of the isotherms and streamlines plots.

Figure 3a-e show the computed streamlines when the inclination angle is varied from 20° to 90°. As can be seen form Fig. 3a, the streamlines are rectangular in shape when the hot wall is at a right angle with respect to the horizontal axis. The air near the hot wall is heated and goes up due to the buoyancy effect before it curves up following the shape of the sidewall. Then as it is cooled by the cold wall, the air gets heavier and goes downwards to complete the cycle.

There are two types of cells captured namely the primary and secondary vortices. The primary vortex is transformed from a double cellular shape at higher
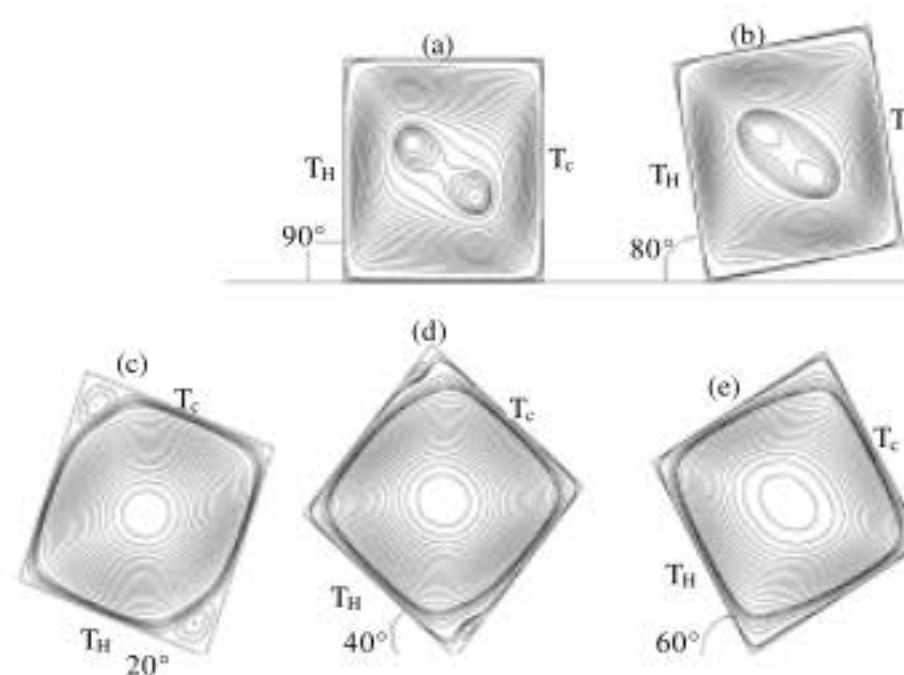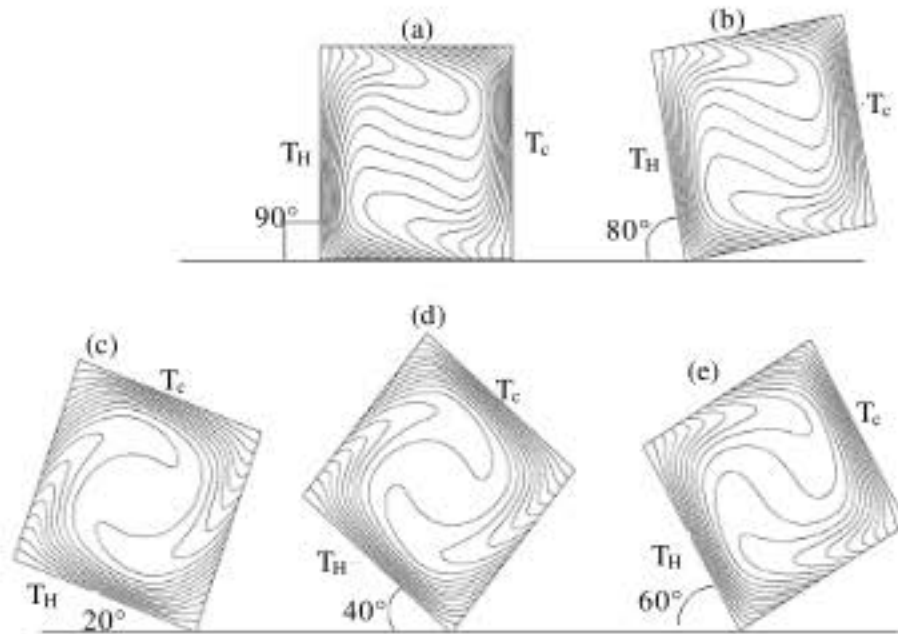

Fig. 3: (a-e) Streamline plots

Fig. 4: (a-e) Isotherms plot

Fig. 5: Plot of average Nusselt number vs. inclination angle

inclination angle (Fig. 3a) to a single cellular shape (Fig. 3e) at low inclination angle. When the hot wall is normal to the horizontal axis, there is no gravity component acting on the fluid along the sidewalls. As the cavity is inclined, the gravity component started to act along the sidewalls and assists the flow. The acceleration of the flow can be seen along the walls from angle 60° and lower, which cause the transformation of the primary. On the other hand, the secondary vortex are captured at inclination angle of 20° and 40°.

Figure 4a-e show the plots of isotherms for every simulation conditions. They demonstrate a denser collection of isotherms near the isothermal walls indicates high heat transfer rate at this region. The domination of vertical isotherms which are parallel with the hot and cold walls is reduced as the inclination angle varies from 20° to 90°. Qualitatively, it may be deduced from the isotherms that as the inclination angle increases, the convection mode of heat transfer dominates over the conduction mode.

The effect of the inclination angle on the Nusselt number is investigated and demonstrates in Fig. 5. As can be seen from the Fig. 5, the average Nusselt number on the hot and cold walls reaches its maximum value at the inclination angle of around 65°. This seems to be a 'critical angle' where the natural convection is at the maximum point. This phenomenon can be explained by referring to Fig. 3 that for an inclination angle greater than 60°, the primary vortex is transformed from a single cellular to a double cellular structure and the cell size is getting bigger. Thus, more fluid is circulating at the centre of the cavity which does not reach either hot wall or cold wall which decreases the natural convection heat transfer mechanism.
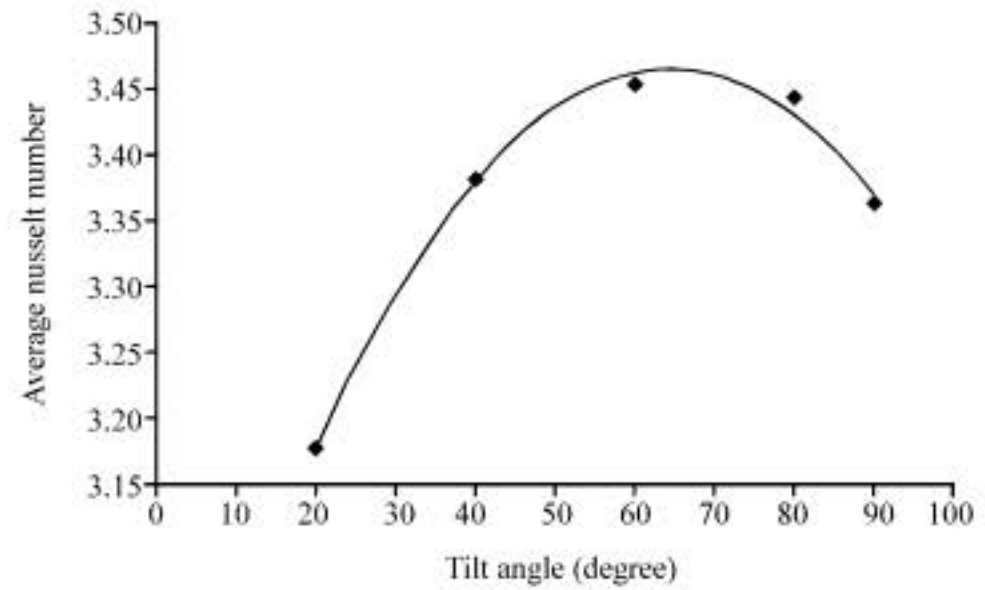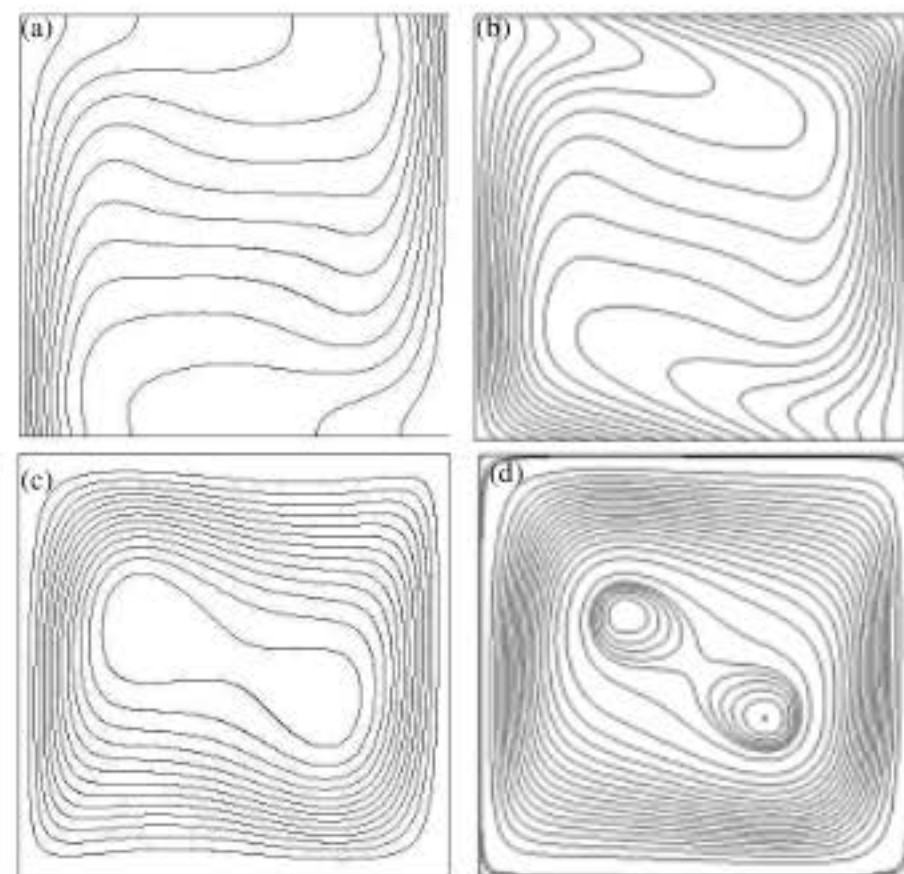

Fig. 6: (a-d) Comparison of plots of isotherms and streamlines between for adiabatic and perfectly conducting boundary conditions

The conduction effect can be seen clearly in the isotherms plots (Fig. 4). The direction of air movement in the streamlines is in agreement with the isotherms shifts that are captured in the isotherms result. Since, the convection is mainly driven by the movement of fluids, the advection of air triggers the convection heat transfer and moves the constant temperature line in the direction of its motion.

Moreover, the effect of boundary condition can be seen clearly from the comparison between the isotherms plot of the present study and that of by Azwadi and Tanahashi (2006) as shown in Fig. 6a-d. Even though the general pattern of the temperature lines is similar, however, there is a significant variation along the

sidewalls. The rate of change of temperature of the present study is more constant compare to the study with adiabatic boundary condition. This is expected since the perfectly conducting boundary condition is defined based on the linear decrease of the temperature from the hot wall to the cold wall. On the other hand, from the comparison of streamline plots, the perfectly conducting boundary condition does not show any significant effect on the flow behavior.

CONCLUSION

The natural convection in an inclined cavity had been simulated using finite difference approach where the Navier Stokes equation had been modified in terms of vorticity and stream function. The result of streamlines plots clearly depicting the flow pattern and vortex structure in the cavity. On the other hand, the isotherms plot has captured the isothermal lines pattern that indicates the dominant mode of heat transfer mechanism and the region of high heat transfer rate. Based on the isotherms plot, the heat transfers near the isothermal walls are higher compared to the other parts in the cavity. The primary vortex is transformed from a single cellular to a double cellular as the inclination angle increases. In addition, the natural convection increases as the inclination angel increases until it reaches the critical angle after which the natural convection starts to decrease. Based on the average Nusselt number, we found that the maximum natural convection occurs in the region of 65° inclination angle. Moreover, the perfectly conducting boundary condition shows significant effect on the isotherms along the sidewalls where a linear change of temperature is captured.

ACKNOWLEDGMENT

REFERENCES

Azwadi, C.S.N. and T. Tanahashi, 2006. Simplified thermal lattice Boltzmann in incompressible limit. Intl. J. Mod. Phys. B., 20: 2437-2449.

Azwadi, C.S.N. and T. Tanahashi, 2007. Three-dimensional thermal lattice Boltzmann simulation of natural convection in a cubic cavity. Int. J. Mod. Phys. B., 21: 87-96.

Azwadi, C.S.N. and T. Tanahashi, 2008. Simplified finite difference thermal lattice Boltzmann method. Int. J. Mod. Phys. B., 22: 3865-3876.

Bubvonich, V., C. Rosas, R. Santander and G. Caceras, 2002. Computation of transient natural convection in a square cavity by an implicit finite-difference scheme in terms of the stream function and temperature. Numer. Heat Transfer Part A: Appl., 42: 401-425.

Clifton, J.V. and A.J. Chapman, 1969. Natural-convection on a finite-size horizontal plate. Int. J. Heat Mass Transfer, 12: 1573-1584.

Das, M.K. and K.S.K. Reddy, 2006. Conjugate natural convection heat transfer in an inclined square cavity containing a conducting block. Int. J. Heat Mass Transfer, 49: 4987-5000.

Ha, M.Y. and M.J. Jung, 2000. A numerical study on three-dimensional conjugate heat transfer of natural convection and conduction in a differentially heated cubic enclosure with a heat-generating cubic conducting body. Int. J. Heat Mass Transfer, 43: 4229-4248.

Ha, M.Y., I.K. Kim, H.S. Yoon, K.S. Yoon, J.R. Lee, S. Balachandar and H.H. Chun, 2002. Two dimensional and unsteady natural convection in a horizontal enclosure with a square body. Numer. Heat Transfer Part A: Appl., 41: 183-210.

Hart, J.E., 1971. Stability of the flow in a differentially heated inclined box. J. Fluid Mech., 47: 547-576.

Hassan, K.E. and S.A. Mohamed, 1970. Natural convection from isothermal flat surfaces. Int. J. Heat Mass Transfer, 13: 1873-1886.

Hiroyuki, O., K. Yammamoto, S. Hayatoshi and S.W. Churchill, 1974. Natural convection in an inclined rectangular channel heated on one side and cooled on the opposing side. Int. J. Heat Mass Transfer, 17: 1209-1217.

Kim, D.M. and R. Viskanta, 1984. Study of the effects of wall conductance on natural convection in differentially oriented square cavities. J. Fluid Mech., 144: 153-176.

Kuyper, R.A., T.H.H. van der Meen, C.J. Hoogendoorn and A.A.W.M. Henkes, 1993. Numerical study of laminar and turbulent natural convection in an inclined square cavity. Int. J. Heat Mass Transfer, 36: 2899-2911.

Lee, S.L. and J.M. Hellman, 1969. Study of firebrand trajectories in a turbulent swirling natural convection plume. J. Combustion Flame, 13: 645-655.

Oosthuizen, P.H. and D. Naylor, 1998. Introduction to Convective Heat Transfer Analysis. McGraw-Hill Book Co., New York.

Ostrach, S., 1988. Natural convection in enclosures. J. Heat Trans. ASME, 110: 1175-1190.

Qi, H.D., 2008. Fluid flow and heat transfer characteristics of natural convection in a square cavities due to discrete source-sink pairs. Int. J. Heat Mass Transfer, 51: 5949-5957.

Rasoul, J. and P. Prinos, 1997. Natural convection in an inclined enclosure. Int. J. Numer. Method Heat Fluid Flow, 7: 438-478.

Sun, Y.S. and A.F. Amery, 1997. Effects of wall conduction, internal heat sources and an internal baffle on natural convection heat transfer in a rectangular enclosure. Int. J. Heat Mass Transfer, 40: 915-929.

Yucel, N. and H. Ozdem, 2003. Natural convection in partially divided square enclosures. Heat Mass Transfer, 40: 167-175.